Amazon rain forest subcanopy flow and the carbon budget: Santarém LBA–ECO site

Article *in* Journal of Geophysical Research Atmospheres · March 2008

DOI: 10.1029/2007JG000597 · Source: OAI

8 authors, including:

Julio Tota
Universidade Federal do Oeste do Pará
109 PUBLICATIONS **1,762** CITATIONS
SEE PROFILE

David R. Fitzjarrald
University at Albany, The State University of New York
161 PUBLICATIONS **7,449** CITATIONS
SEE PROFILE

Ralf M. Staebler
Environment and Climate Change Canada
196 PUBLICATIONS **5,888** CITATIONS
SEE PROFILE

Ricardo Sakai
Howard University
59 PUBLICATIONS **1,279** CITATIONS
SEE PROFILE

JOURNAL OF GEOPHYSICAL RESEARCH, VOL. 113, G00B02, doi:10.1029/2007JG000597, 2008

Amazon rain forest subcanopy flow and the carbon budget: Santarém LBA-ECO site

Julio Tóta,[1] David R. Fitzjarrald,[2] Ralf M. Staebler,[3] Ricardo K. Sakai,[2] Osvaldo M. M. Moraes,[4] Otávio C. Acevedo,[4] Steven C. Wofsy,[5] and Antonio O. Manzi[1]

Received 17 September 2007; revised 3 March 2008; accepted 22 May 2008; published 22 July 2008.

[1] Horizontal and vertical CO_2 fluxes and gradients were made in an Amazon tropical rain forest, the Tapajós National Forest Reserve (FLONA-Tapajós: 54°58′W, 2°51′S). Two observational campaigns in 2003 and 2004 were conducted to describe subcanopy flows, clarify their relationship to winds above the forest, and estimate how they may transport CO_2 horizontally. It is now recognized that subcanopy transport of respired CO_2 is missed by budgets that rely only on single point eddy covariance measurements, with the error being most important under nocturnal calm conditions. We tested the hypothesis that horizontal mean transport, not previously measured in tropical forests, may account for the missing CO_2 in such conditions. A subcanopy network of wind and CO_2 sensors was installed. Significant horizontal transport of CO_2 was observed in the lowest 10 m of the canopy. Results indicate that CO_2 advection accounted for 73% and 71%, respectively, of the carbon budget for all calm nights evaluated during dry and wet periods. We found that horizontal advection is likely important to the canopy CO_2 budget even for conditions with the above-canopy friction velocity higher than commonly used thresholds.

Citation: Tóta, J., D. R. Fitzjarrald, R. M. Staebler, R. K. Sakai, O. M. M. Moraes, O. C. Acevedo, S. C. Wofsy, and A. Manzi (2008), Amazon rain forest subcanopy flow and the carbon budget: Santarém LBA-ECO site, *J. Geophys. Res.*, *113*, G00B02, doi:10.1029/2007JG000597.

1. Introduction

[2] In the last decade tower-based eddy-covariance (EC) observations have been established worldwide to monitor net ecosystem exchange (NEE) of carbon dioxide [*Goulden et al.*, 1996; *Black et al.*, 1996; *Baldocchi et al.*, 2001]. This micrometeorological method is considered the most accurate when applied at nearly flat sites that have long homogeneous upwind fetches. Its application has spawned global scale flux-measuring networks [*Baldocchi et al.*, 1988; *Aubinet et al.*, 2000] whose justification has been to estimate long-term carbon exchange. Two related issues complicate this ambition. First, proper estimates of nocturnal respiratory fluxes are essential, but weak turbulent mixing at night is common. This issue of underreporting of nocturnal CO_2 fluxes has been addressed using the approach advocated by *Goulden et al.* [1996], formalized by the FLUXNET committee [*Baldocchi et al.*, 2001]. Data on very calm nights (often an appreciable fraction of all nights) is simply discarded and replaced with the result of an ecosystem respiration rate found on windy nights that are otherwise similar [*Miller et al.*, 2004; *Gu et al.*, 2005]. A second issue is that many flux-observing sites lie in complex terrain [*Lee*, 1998; *Paw U et al.*, 2000; *Aubinet et al.*, 2003; *Feigenwinter et al.*, 2004; *Staebler and Fitzjarrald*, 2004, 2005]. On the very calm nights for which flux underestimates occur, subcanopy drainage flows are most common [*Yoshino*, 1984; *Sun et al.*, 2007]. Whether or not subcanopy drainage flows also advect sufficient CO_2 laterally out of the budget "box" to account for the 'missing flux' on calm nights is site specific, and must be determined observationally [*Lee*, 1998; *Feigenwinter et al.*, 2004; *Staebler and Fitzjarrald*, 2004; *Aubinet et al.*, 2005]. Previous studies show that, under light wind and very stable conditions over the canopy, the importance of advection on the carbon balance can be as large as, or even larger than, the magnitude of NEE, observed by the EC approach when there are drainage flows [*Staebler*, 2003; *Staebler and Fitzjarrald*, 2004, 2005; *Sun et al.*, 2007]. To assess the importance of subcanopy flows one must present a plausible physical mechanism to account for this underestimation as past studies asserted [*Kruijt et al.*, 2004; *Araújo et al.*, 2002]. Even on gentle slopes, it is risky to assume that there

[1]Instituto Nacional de Pesquisas da Amazônia, Manaus, Amazonas, Brazil.
[2]Atmospheric Sciences Research Center, University at Albany, State University of New York, Albany, New York, USA.
[3]Air Quality Research Branch, Environment Canada, Toronto, Ontario, Canada.
[4]Departamento de Física, Universidade Federal de Santa Maria, Santa Maria, Rio Grande do Sul, Brazil.
[5]Department of Earth and Planetary Sciences, Harvard University, Cambridge, Massachusetts, USA.

0148-0227/08/2007JG000597$09.00

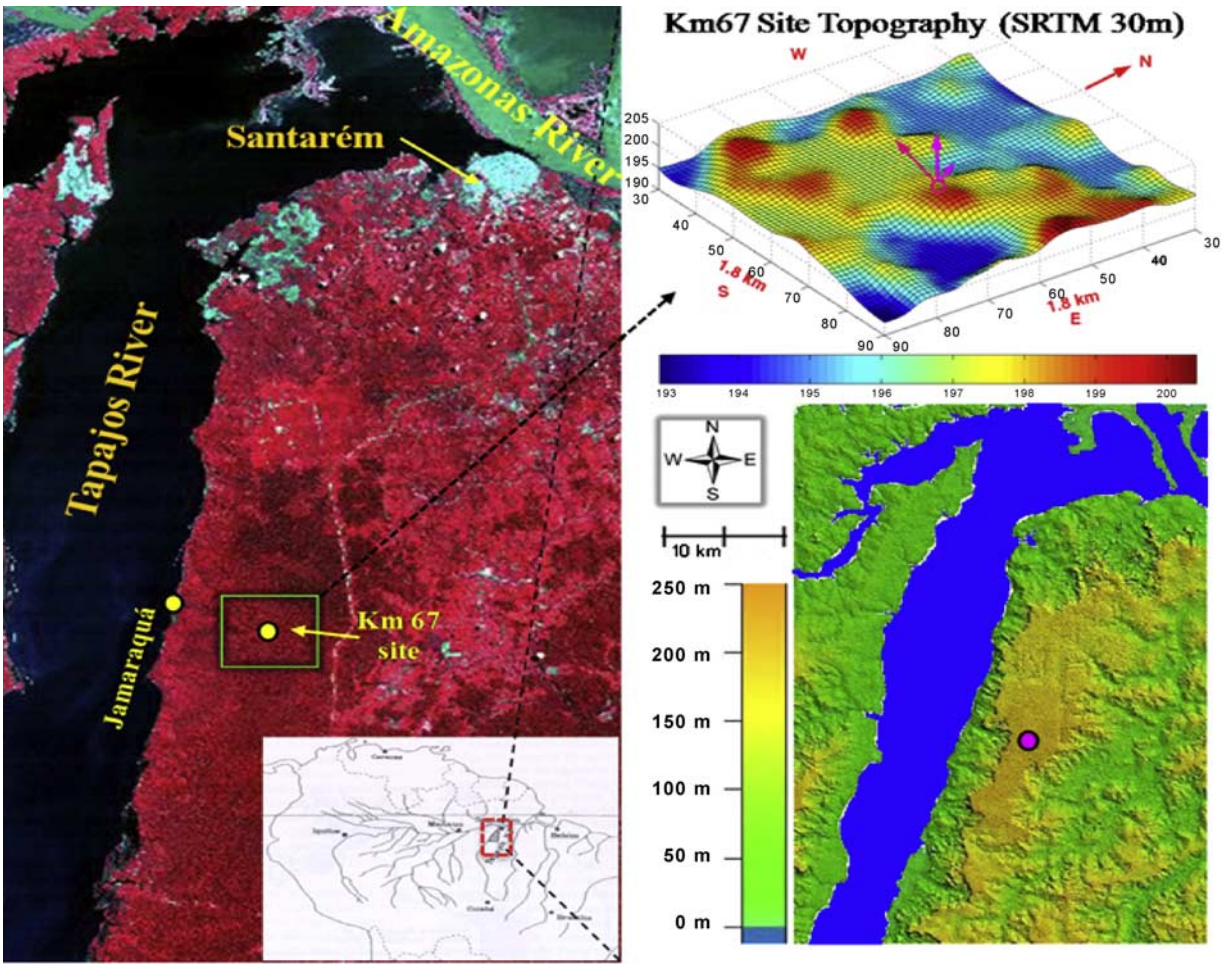

Figure 1. Site Location in the vegetation cover image and high resolution (30 m grid space) tower-base local topography as determined by the Shuttle Radar Topography Mission (SRTM). The arrows shows the modal wind direction at 57.8 m (red, from east) and in the subcanopy (magenta, from southeast).

is no lateral motion or divergence that can advect CO_2 and applying the ideal site criteria to more typical situations is questionable [*Baldocchi et al.*, 2000; *Staebler and Fitzjarrald*, 2004, 2005].

[3] Most studies of subcanopy advection to date have been done at midlatitude sites. We are not aware of similar studies in the tropical rain forest. The forests in the Amazon region account for 10% of the world's terrestrial primary productivity and about the same fraction of carbon stored in land ecosystems [*Malhi et al.*, 1998]. In the last decade reports have suggested that this region has such a positive sink of CO_2, which, when scaled for the entire Amazon region, could account for a significant fraction of the missing carbon budget. Since results from the Large Scale Biosphere-Atmosphere experiment in Amazonia (LBA [*Keller et al.*, 2004]) will likely be used to represent the Amazon in its entirety in global change models, it is important to identify systematic observation problems. In this paper we describe a detailed subcanopy CO_2 and wind system sensors deployed for the first time in the Amazon tropical rain forest combined with EC tower flux and respiration measurements and analyze the results with the aim to better understand the local carbon budget. Formally, we test the hypotheses that EC measurements underestimate the CO_2 flux on calm nights because of lateral airflow out of the control volume at the km67 Santarém LBA site. We seek to demonstrate that observed subcanopy horizontal CO_2 gradients and wind transport processes yield significant mean net transport of CO_2 into or out of the control volume. Following *Staebler and Fitzjarrald* [2004, 2005], we examine the importance of subcanopy advection in the following steps: (1) We must show that systematic subcanopy flows exist and are measurable; and (2) observed subcanopy flows must be related to a physical driving mechanism (e.g., drainage forcing) that ensures that they are sufficiently systematic so that long-term budgets are affected.

2. Material and Methods

2.1. Site Description

[4] The study site (54°58′W, 2°51′S) is part of the ecological component of the Large Scale Biosphere-Atmosphere experiment in Amazonia (LBA-ECO), which aims to achieve better understanding of the regional carbon balance. It is located in the Tapajós National Forest reserve (FLONA Tapajós), near km 67 of the Santarém-Cuiabá highway (BR-163). The average temperature, humidity, and rainfall

Table 1. LBA – Old Growth (KM67) Site Sensors

Level (m)	Parameter	Instrument
64.1, 52, 38.2, 30.7	Wind speed	Cup anemometers
57.8	u′ v′ w′ T′,CO_2, H_20	CSAT 3D sonic anemometers LI-7000 CO_2/H_20 analyzers
5	U′ v′ w′ T′	ATI 3D sonic anemometer
1.8	CO_2, U, V, T (horizontal array)	CATI/2 2D sonic anemometers, LI-7000
62.2, 50.1, 39.4, 28.7 19.6, 10.4, 3.1, 0.9	CO_2, H_20 Profile	LI-7000 CO_2/H_20 analyzer
61.9, 49.8, 39.1, 28.4 18.3, 10.1, 2.8, 0.6	Temperature	Aspirated thermocouples

are 25.8°C, 85%, and about 1800 mm per year, respectively [*Parotta et al.*, 1995]. This area contains predominantly nutrient-poor clay oxisols with some sandy utisols [*Silver et al.*, 2000], each of which has low organic content and cation exchange capacity.

[5] Vegetation consists of occasional 55 m height emergent trees with a closed canopy at 40 m and below [*Parker and Fitzjarrald*, 2004]. Trees include *Manilkara huberi* (Ducke) *Chev., Hymenaea courbaril L., Betholletia excelsa Humb*. and *Bonpl.*, and *Tachigalia spp* species, and epiphytes. There is overall an uneven age distribution, but the forest can be considered to be primary or old growth [*Clark*, 1996; *Goulden et al.*, 2004].

[6] Local topographic features include a steep nearby river escarpment sloping to the Tapajós River to the west, but with a weak eastward-facing slope into the basin of the Curua-Una watershed. Except near the escarpment, drainage flows would be expected to move opposing the easterly prevailing wind field (red arrow in the Figure 1).

[7] Several studies have demonstrated strong seasonal variations in solar radiation, net radiation, air temperature, and vapor pressure deficit, all of which increase substantially with the seasonal decline in precipitation, while surface litter and soil moistures also decline [*da Rocha et al.*, 2004].

2.2. Instrumentation and Observation

[8] The field measurements at the old growth forest site at km67 in the LBA study area included several meteorological and EC measurements from 2001 though 2006, focusing on the dynamics of primary forest ecosystems. Several LBA groups have made observations of meteorological quantities, such as EC fluxes of H_2O, CO_2, temperature, and wind fields. We share data sets obtained by the LBA Project groups CD03 and CD10 (CD - Carbon Dynamics).

[9] The CD10 tower systems include EC and meteorological wind, CO_2, temperature and water vapor profiles collected between 2001 and 2006 (Table 1 and Figure 2). The instrumentation descriptions and quality control procedures for the basic data sets obtained at the main km67 tower site are given by *Saleska et al.* [2003] or at the online

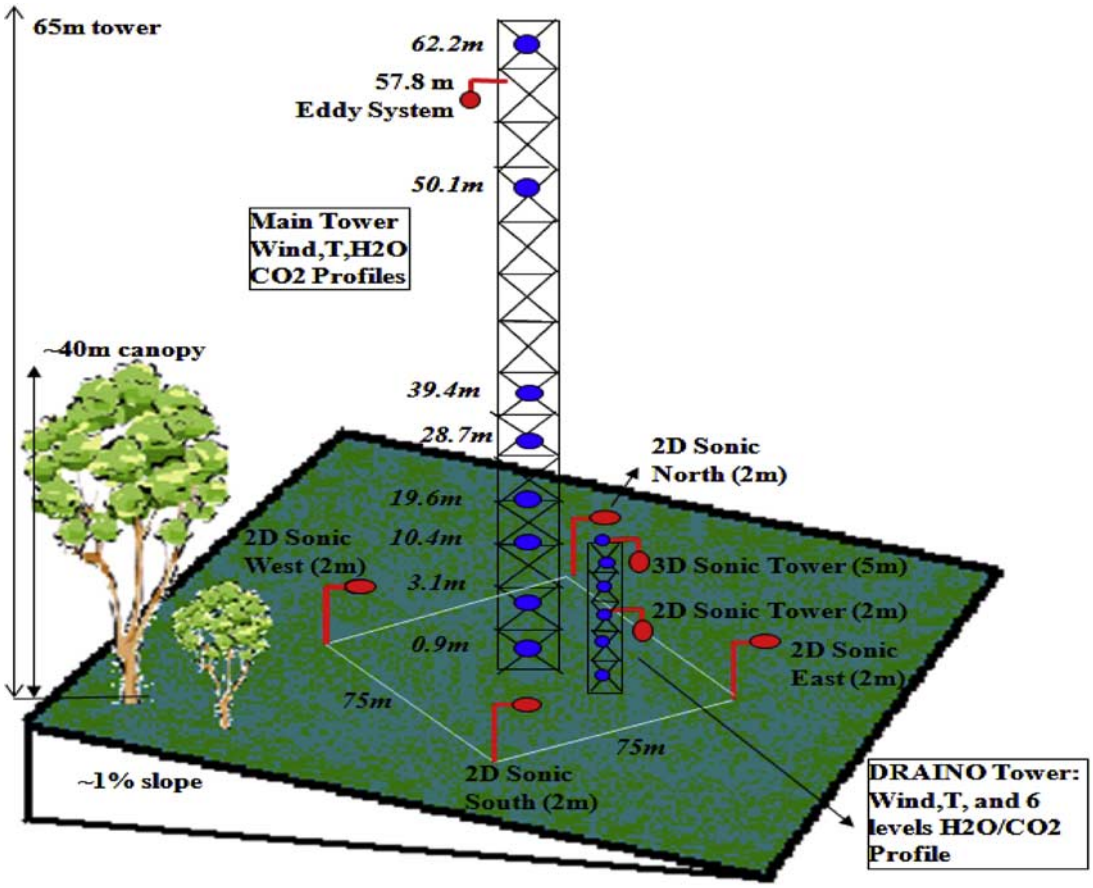

Figure 2. Main tower and Draino deployed instruments systems.

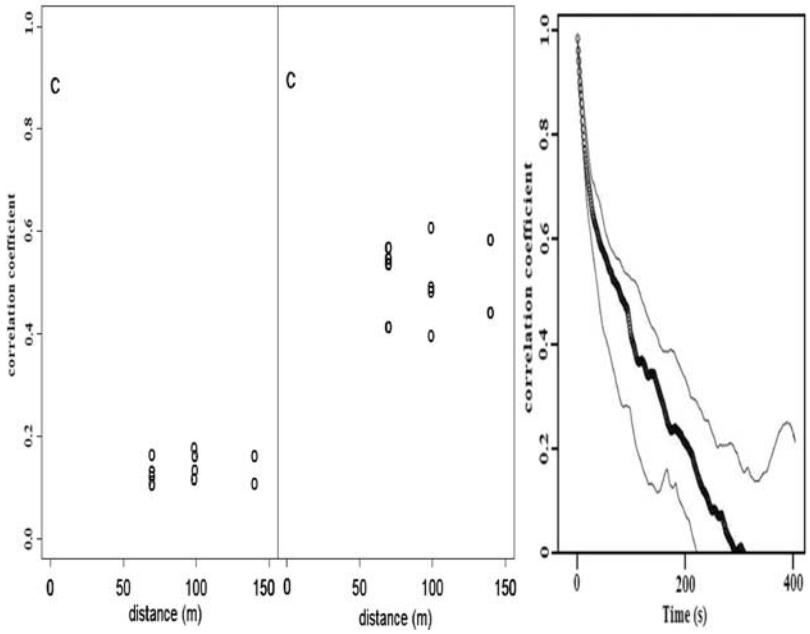

Figure 3. The autocorrelation coefficient for total wind speed (left) and CO_2 concentration (middle) as a function of distance between sampling points 1.8 m above ground in the subcanopy. (3-min averages data from "Draino" Phase 1 (DOY 198-238/2003). "C" represents the calibration period. (right) Temporal autocorrelation. The solid line represents the median, and the thinner lines represent the upper and lower quartiles. Mean wind speed in the subcanopy was 0.13 m/s.

web page http://www-as.harvard.edu/data/lbadata.html. A weather station was deployed in Jamaraquá at the base of the Tapajós escarpment to help in identifying topographical effects. A high resolution STRM map was made, based on a 90 m grid, interpolated to 30 m, to describe the gentle topography around the tower site (Figure 1).

[10] Subcanopy network observations are available for two campaigns in 2003 (Phase 1, DOY 198-238) and 2004/2005 (Phase 2, DOY 250-366 and 01-32). The subcanopy data complement observations that were made around the central 65-m tower. The observation and acquisition approach was developed at ASRC (*Staebler and Fitzjarrald*, 2005) and includes a PC operating in Linux, an outboard Cyclades multiple serial port (CYCLOM-16YeP/DB25) collecting and merging serial data streams from all instruments in real time, with the data archived into 12-h ASCII files. Observations include CO_2, temperature, H_2O and wind field measurements at 1 Hz (Figure 2). The system included a LI-7000 Infrared Gas Analyzer (LI-COR inc., Lincoln, Nebraska, USA), a multiposition valve (Vici Valco Instrument Co., Inc.) controlled by a CR23x Micrologger (Campbell Scientific, Inc., Logan, Utah, USA), which also monitored flow rates. The instrument network array (Figure 2 and Table 1) consisted of 6 subcanopy sonic anemometers: a Gill HS (Gill Instruments Ltd., Lymington, UK) 3-component sonic anemometer at 5 m elevation in the center of the grid and 5 SPAS/2Y (Applied Technologies Inc., CO, USA) 2-component anemometers (1 sonic at center and 4 sonic along the periphery), with a resolution of 0.01 m s^{-1}. The horizontal gradients of CO_2/H_2O were measured in the array at 2 m above ground, by sampling sequentially from 4 horizontal points surrounding the main tower location at distances of 70-80 m, and from points at 6 levels on the small Draino tower, performing a 3-min cycle. Air was pumped continuously through 0.9 mm Dekoron tube (Synflex 1300, Saint-Gobain Performance Plastics, Wayne, NJ, USA) tubes from meshed inlets to a manifold in a centralized box. A baseline airflow of 4 LPM from the inlets to a central manifold was maintained in all lines at all times to ensure relatively "fresh" air was being sampled. The air was pumped for 20 s from each inlet, across filters to limit moisture effects. The delay time for sampling was 5 s, and the first 10 s of data were discarded. At the manifold, one line at a time was then sampled using an infrared gas analyzer (LI-7000, Licor, Inc.). The 6-level CO_2 profile on the 5 m tower was determined in a similar, sequential manner, using a LI-7000 gas analyzer sampling pumped air from all 10 points (6 vertical, 4 horizontal) in the measurement array. Flow rates at the inlets were checked regularly to ensure proper flow and to detect potential leaks.

2.3. Preinstallation Intercomparison

[11] Following *Staebler and Fitzjarrald* [2004] an initial instrument intercomparison was made to identify the performance of the integrated subcanopy observation system. The CO_2 sensor (Licor 7000 sensor) and the sonic anemometers (CATI/2 and SPAS/2Y, Applied Technologies, Inc. sensors) were co-located on the small tower for a calibration period (5 d) before being deployed at 1.8 m above the ground (Figure 2). We anticipated that the horizontal transport product *uc* would be near its largest value at this height, a finding later confirmed at this site (see Figure 4 below). We had insufficient instrumentation to construct a network of towers to measure the CO_2 concentration up to canopy top, and this led us to continue our earlier practice of asserting a profile similarity hypothesis

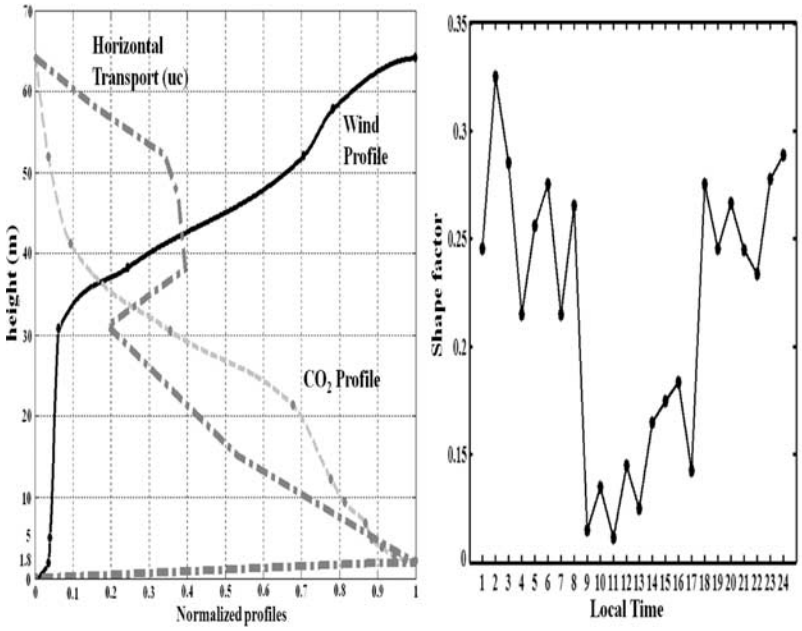

Figure 4. Typical nighttime normalized median profiles of CO_2, wind speed and their product (*uc*) horizontal transport (left); and the diurnal cycle of the shape factor for horizontal advection (right).

(see next section). Using a single gas analyzer with a common path multiposition valve for the horizontal and vertical profiles minimizes the potential for systematic concentration errors. A field calibration was performed by co-locating sensors and gas inlets at the same point of measurement. The comparisons indicate scatter in $[CO_2]$ because samples were sequential, not synchronous. The mean standard error was <0.05 ppm. The wind comparisons were made using a 3D sonic as the standard for the 2D sonic anemometers, resulting in a mean standard error of about 0.005 ms^{-1}. Ambient subcanopy wind speed was on the order of a few cm s^{-1} and can be reliably measured in the subcanopy space by the system. After intercomparison, the sonic anemometers and the CO_2 inlet tubes were moved from the small tower center point and deployed about 2 m above ground as indicated in Figure 2.

[12] We examined to what extent the subcanopy sensor geometry of CO_2 allows the system to function as a network, whether the network can be used to capture the relevant gradients and transport processes in very low wind conditions [*Staebler and Fitzjarrald*, 2004]. Figure 3 (left) shows the 3-min data autocorrelation of CO_2 and wind fields determined from continuous measurements. The relevant spatial scale X is approximately 70–150 m. We assessed our choice of network size by examining observed spatial and temporal autocorrelations. The spatial autocorrelation of horizontal wind speed drops rapidly to 0.2 in 60 m, but fluctuations in CO_2 exhibit a larger integral scale 100–200 m while the temporal integral is approximately 100–300 s (Figure 3, right). This is consistent with results obtained by *Staebler and Fitzjarrald* [2004] in a very different forest, except that the characteristic horizontal CO_2 scale is larger than that at Harvard Forest, consistent with the thicker canopy at the Tapajós National Forest. We do not understand why the spatial correlations do not decrease with increasing distance, as was observed in *Staebler and Fitzjarrald* [2004]. This could be a consequence of the temporal scale variations being larger than are the spatial ones.

2.4. CO_2 Conservation Equations

[13] The net ecosystem exchange (NEE) for a horizontal plane at height h, which represents the exchange rate between forest and atmosphere, is given by,

$$NEE_h = F_0 + \int_0^h \bar{s} dz, \tag{1}$$

where F_0 is the soil flux entering (or leaving) the control volume at the bottom and the $\bar{s}$ integral describes the sum of all sources and sinks in the canopy space. The Reynolds average conservation equation of a scalar "c," ignoring molecular diffusion process, can be expressed by,

$$\frac{\partial \bar{c}}{\partial t} + \bar{u}_i \frac{\partial \bar{c}}{\partial x_i} + \bar{c} \frac{\partial \bar{u}_i}{\partial x_i} + \frac{\partial \overline{u_i' c'}}{\partial x_i} = \bar{s}, \tag{2}$$

with $\bar{u}_i = (u,v,w)$. Considering using equations (1) and (2), and considering incompressibility, after integrating vertically, it can be written in the form,

$$\underbrace{\int_0^h \frac{\partial \bar{c}}{\partial t} dz}_{[1]} + \underbrace{\int_0^h \bar{u} \frac{\partial \bar{c}}{\partial x} dz}_{[2]} + \underbrace{\int_0^h \bar{v} \frac{\partial \bar{c}}{\partial y} dz}_{[3]} + \underbrace{\int_0^h \bar{w} \frac{\partial \bar{c}}{\partial z} dz}_{[4]} + \underbrace{\int_0^h \frac{\partial \overline{u'c'}}{\partial z} dz}_{[5]} + \underbrace{\int_0^h \frac{\partial \overline{v'c'}}{\partial z} dz}_{[6]} + \underbrace{\left(\overline{w'c'}\right)_h}_{[7]} = \underbrace{\int_0^h \bar{s} dz}_{[8]}, \tag{3}$$

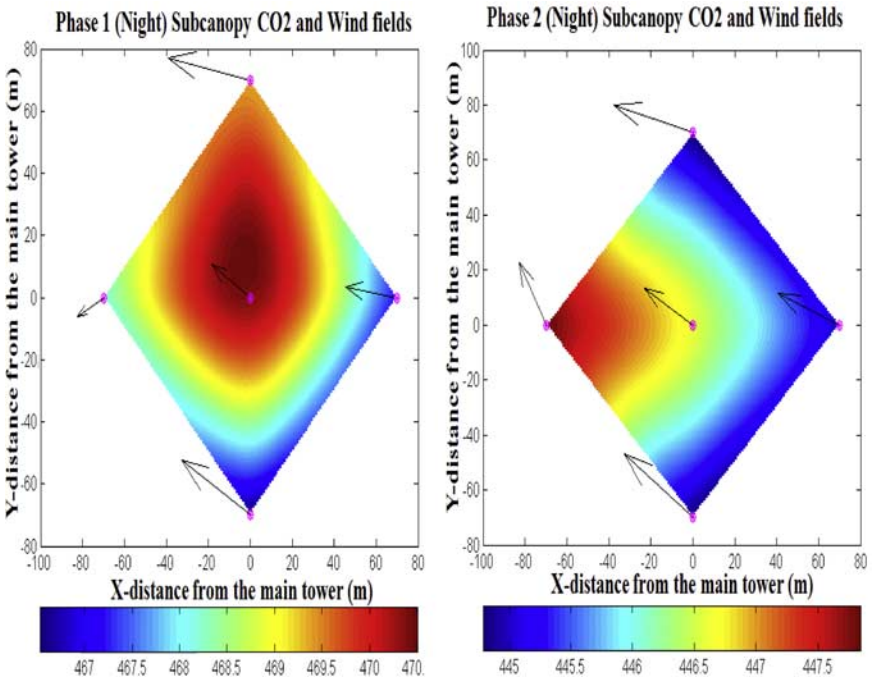

Figure 5. Nighttime composite of averaged subcanopy CO_2 concentration field and wind vectors for Phase 1 and Phase 2 campaigns. The units are in ppm and m s^{-1}, respectively. (Largest arrow is 0.15 m s^{-1}.)

where u, v, and w, are wind components and "c" a scalar, such as CO_2. The term [4] is the vertical advection term and term [8] the sum of all sinks and sources between $z = 0$ and $z = h$, including everything crossing the lower boundary at $z = 0$.

[14] In the case of horizontal homogeneity, terms [1], storage in the canopy space, and [7], vertical eddy flux at $z = h$ (57.8 m for the site studied), are obtained from standard EC and profile sensors at the flux site. Terms [5] and [6] are the horizontal turbulent flux divergence and negligible when compared with other terms [*Yi et al.*, 2000; *Turnipseed et al.*, 2003]. The terms [2], [3] and [4] respectively are horizontal and vertical advection.

[15] The vertical mean advection was integrated using the method of *Lee* [1998]:

$$[\overline{wc}]_0^h - \frac{\bar{w}_h}{h}\int_0^h \bar{c}(z)dz = \bar{w}_h\left(\bar{c}(h) - \frac{1}{h}\int_0^h \bar{c}(z)dz\right), \qquad (4)$$

where $\bar{w}_h$ and $\bar{c}(h)$ are the residual vertical velocity and the mean concentration at the top of the layer (57 m), respectively [see *Staebler and Fitzjarrald*, 2004]. *Staebler and Fitzjarrald* [2004] argued that Lee's approach is an overestimate, noting that the assumption of a linear increase of $\bar{w}_h$ with height is often violated. Comparisons of the divergence measurements at 1.8 m height with measured vertical velocities at 46 m and 57.8 m were made for a few days of wind data and the results show no correlation indicating that Lee's approach is also violated for the site studied here. However, Lee's formulation will be used to provide an upper estimate of the vertical advection term in order to compare its potential significance relative to the other terms. The calculation of mean vertical advection was made only during phase 2 (DOY 250–366/2004 and 01–32/2005) when sufficient data for the calculation was available. We recognize that obtaining credible mean vertical velocity from sonic anemometers is still a challenge [e.g., *Vickers and Mahrt*, 2006]. However, the difficulties in assessing one term in the continuity equation should not preclude efforts to obtain the others.

2.5. Vertical Integration of the Horizontal Advection Terms

[16] To perform a complete three-dimensional forest CO_2 box budget it is necessary to obtain vertical profiles of the horizontal gradient measurements for the entire control volume, and this is generally not feasible. We lacked resources to install a network of towers to measure the CO_2 profile at a number of locations in the canopy. Noting, as in *Staebler and Fitzjarrald* [2004], that the product uc is largest near the forest floor, we relied on subcanopy measurements made 1.8 m above the ground. To compensate for the missing network of vertical profiles, we approximate the vertical integration through the canopy of the horizontal advective terms [2] and [3] following methods developed by *Staebler and Fitzjarrald* [2004]. One hypothesizes spatial similarity between vertical CO_2 and wind profiles and their product (the horizontal transport) uc, where u is the average wind and c the average CO_2 concentration. In this assumption, the shapes of the profiles throughout the canopy space are considered similar to the central point where the profiles are measured (Figure 2). Figure 4 presents a typical feature of the shape factor profiles of CO_2 concentration, wind and horizontal transport. The horizontal subcanopy measurement height (1.8 m) is a height where the advection term is expected to be significant, providing confidence for single level height measurements to determine the integrated layer advection.

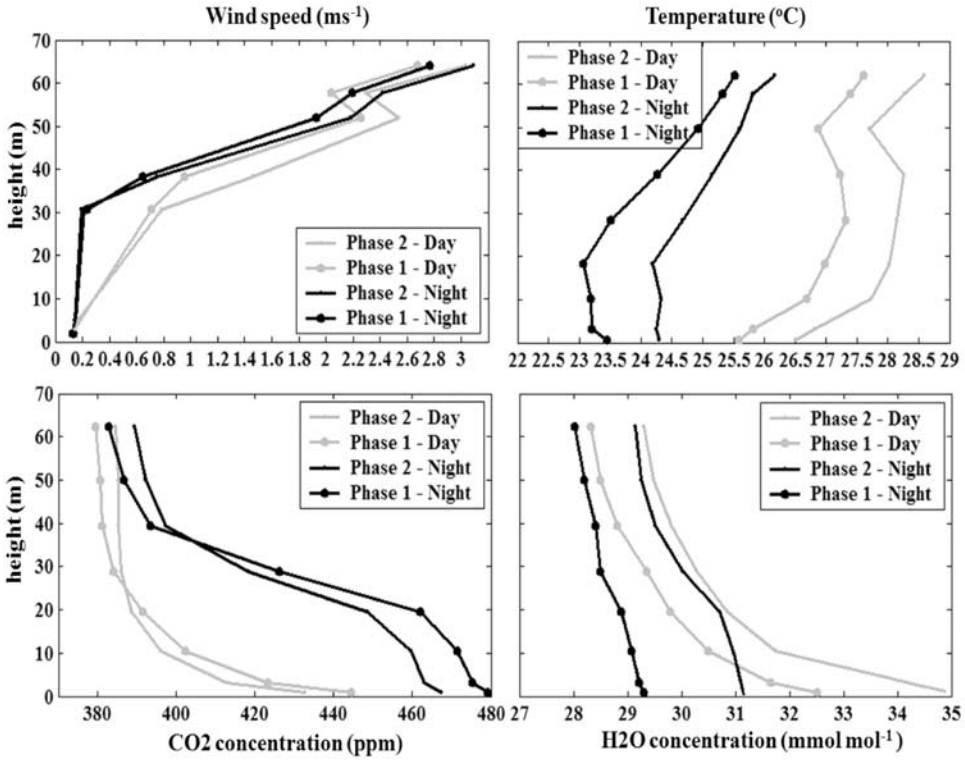

Figure 6. Vertical profiles of concentration of CO_2, wind speed, temperature, and water vapor, for both phases (dry and wet).

[17] The procedure of integrating vertically is formalized through,

$$c^*(x,z) = f(z)c^*(x,z_1), \tag{5}$$

where *f(z)* is the (assumed constant) shape of the CO_2 profile relative to height z_1 = 1.8m (horizontal plane). The difference between the actual CO_2 concentration and nocturnal CO_2 concentration above the canopy (baseline value) is defined as $c^*(z) = c(z) - c_0$. The c^* was used instead of c because there is a practical lowest limit of $CO_2 = c_0$, indicative of the atmospheric base state, since it has no effect on the budget. Then, the vertical integration gives:

$$\int_0^h \frac{\partial c^*(x,z)}{\partial x} dz = \frac{\partial c^*(x,z_1)}{\partial x} \int_0^h f(z)dz = \frac{\partial c^*(x,z_1)}{\partial x} hS_c, \tag{6}$$

where S_c is the shape factor for the CO_2 concentration profile. Applying the same procedure to describe the wind speed profile yields the advection estimates:

$$\begin{aligned}\int_0^h u(x,z)\frac{\partial c^*(x,z)}{\partial x} dz &= \int_0^h g(z)u(x,z_1)f(z)\frac{\partial c^*(x,z_1)}{\partial x} dz \\ &= \left(u(x,z_1)\frac{\partial c^*(x,z_1)}{\partial x}\right)\int_0^h f(z)g(z)dz \\ &= \left(u(x,z_1)\frac{\partial c^*(x,z_1)}{\partial x}\right)\cdot(hS),\end{aligned} \tag{7}$$

where S is the shape factor for horizontal advection of CO_2. The nocturnal time shape factor values for both studied periods averaged 0.28, while the daytime value was typically 0.14 (Figure 4). This is consistent with results obtained by *Staebler and Fitzjarrald* [2004], possibly due to similar shape factors for CO_2 and wind speed profiles at both sites.

3. Results and Discussion

3.1. CO_2 Concentration Field

[18] The average composite of horizontal concentration of CO_2 measured at 2-m height in nocturnal conditions for Phase 1 and Phase 2 (Figure 5) shows that the horizontal CO_2 field varied significantly at night during both observation phases. During Phase 1, the CO_2 concentrations at night were higher than during Phase 2. This may be associated with vegetation response to drier, cooler conditions and lighter wind during this phase, according to Figure 6. The typical values of average horizontal CO_2 gradients were about -0.026 ($\frac{\partial \bar{c}}{\partial x}$, east-west) and 0.023 ($\frac{\partial \bar{c}}{\partial y}$, north-south) ppm m^{-1} for all nights considered (7390 and 18366 average 3-min data values, Phase 1 and Phase 2, respectively). These results are comparable to the range of horizontal CO_2 gradients that have been reported in the literature, 0.025 to 0.079 ppm m^{-1} [*Feigenwinter et al.*, 2004; *Staebler and Fitzjarrald*, 2004; *Aubinet et al.*, 2005]. One expects CO_2 concentrations and gradients near the ground to be site-specific under calm night wind speed conditions, due to varying soil respiration rates that depend on soil and litter layer composition, temperature and moisture.

[19] Vertical profiles of temperature, water vapor concentration, CO_2 concentration and wind speed characterize the

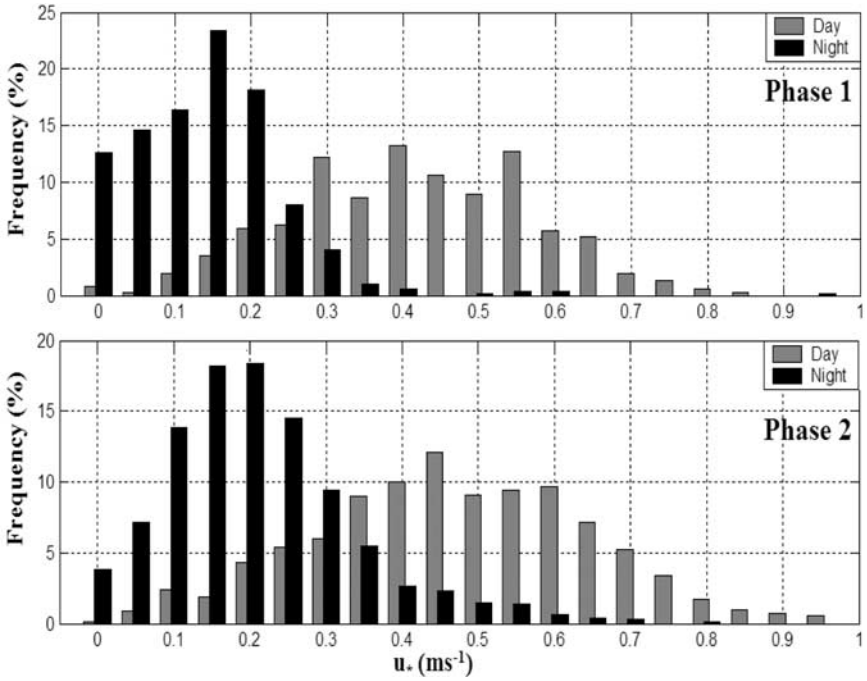

Figure 7. Frequency distribution histogram of friction velocity (u_*) at 57.8 m, for Phase 1 and Phase 2 measurements, separate day and night periods.

microclimate observed during each phase (Figure 6). The drier Phase 1 presents daytime and night patterns that contrast with the wetter Phase 2 conditions. The wind speed profile had a similar shape during both phases, but above the canopy the magnitude of wind speed was greater in Phase 2 compared with Phase 1 period. This suggests a reduction on turbulence level or vertical mixing during the nighttime, as shown in Figure 7. The temperature profiles show the same pattern for the two phases, however, the dry phase was about 2°C warmer. During the daytime, for both dry and wet periods, a maximum air temperature was observed at 30 m associate with the absorption of sunlight by vegetation, generating a light unstable condition between 30 and 50 m, and stable condition below 30 m. During the nighttime the net loss of thermal radiation cooled the vegetation relative to the air adjacent, generating local stability and affecting above-canopy momentum transport. However, from the observed temperature profiles, in the layer below 20 m, trunk space layer, just below the upper canopy; the subcanopy temperature profile was dry and cold relative to the underlying air (≈ -0.25°C m^{-1}). This combination of the cooling above 20 m and warming below generates instability associated with negative buoyancy [see also *Fitzjarrald et al.*, 1990; *Fitzjarrald and Moore*, 1990]. This process may be contributing or creating horizontal flow gravitationally such as suggested by *Lee* [1998]. Similar temperature profiles were reported by *Goulden et al.* [2006] for km83 LBA site 16 km away to the south. As expected, the vertical concentration of CO_2 reflects both atmospheric transport and forest physiological processes, in which during the daytime photosynthesis removes CO_2 from the air depleting concentration levels, and during the nighttime the concentration builds up due to respiration, the reduction of turbulence, and absence of photosynthesis.

[20] The frequency distribution of the friction velocity above the canopy for the both dry (Phase 1) and wet (Phase 2) periods (Figure 7) shows very small values at nighttime. Nocturnal values of friction velocity smaller than 0.2 ms^{-1} accounted for more than 85% and 65% for dry and wet periods, respectively. Therefore, we define deficit nights, using the procedure outlined by *Staebler and Fitzjarrald* [2004], when NEE (CO_2 eddy flux plus storage term) was less than total ecosystem respiration (see *Saleska et al.* [2003] and *Hutyra et al.* [2007] for details of these data sets). About 130 selected nights in each period, Phase 1 and Phase 2 match these criteria and were considered calm nighttime conditions.

[21] Recently, *Saleska et al.* [2003] and *Miller et al.* [2004] have used a cutoff value of 0.3 ms^{-1} for u_* correction to NEE estimates for the site studied. As show in Figure 7, much of the observed data must be discarded using this criterion, possibly altering the results. As reported by *Miller et al.* [2004], the tropical forest in Amazonia becomes a source than sink of atmospheric CO_2 depending of the cutoff value u_* used.

3.2. Subcanopy Horizontal Wind Field

[22] To calculate horizontal advection (terms [3] and [4] in equation (3)), we estimated the horizontal wind field on the subcanopy space using the measurement subcanopy network described above. Though the site was considered flat in earlier reports [*Saleska et al.*, 2003; *Miller et al.*, 2004], a high resolution image shows that the forest floor gently slopes in a west-northwest direction from the main tower, according to Figure 2. *Goulden et al.* [2006] inferred the presence of drainage flows toward the SE at the km83 site to the south of the present study site, but they did not demonstrate subcanopy motion forced by density anomalies. Figure 8 shows statistics of the subcanopy wind field at

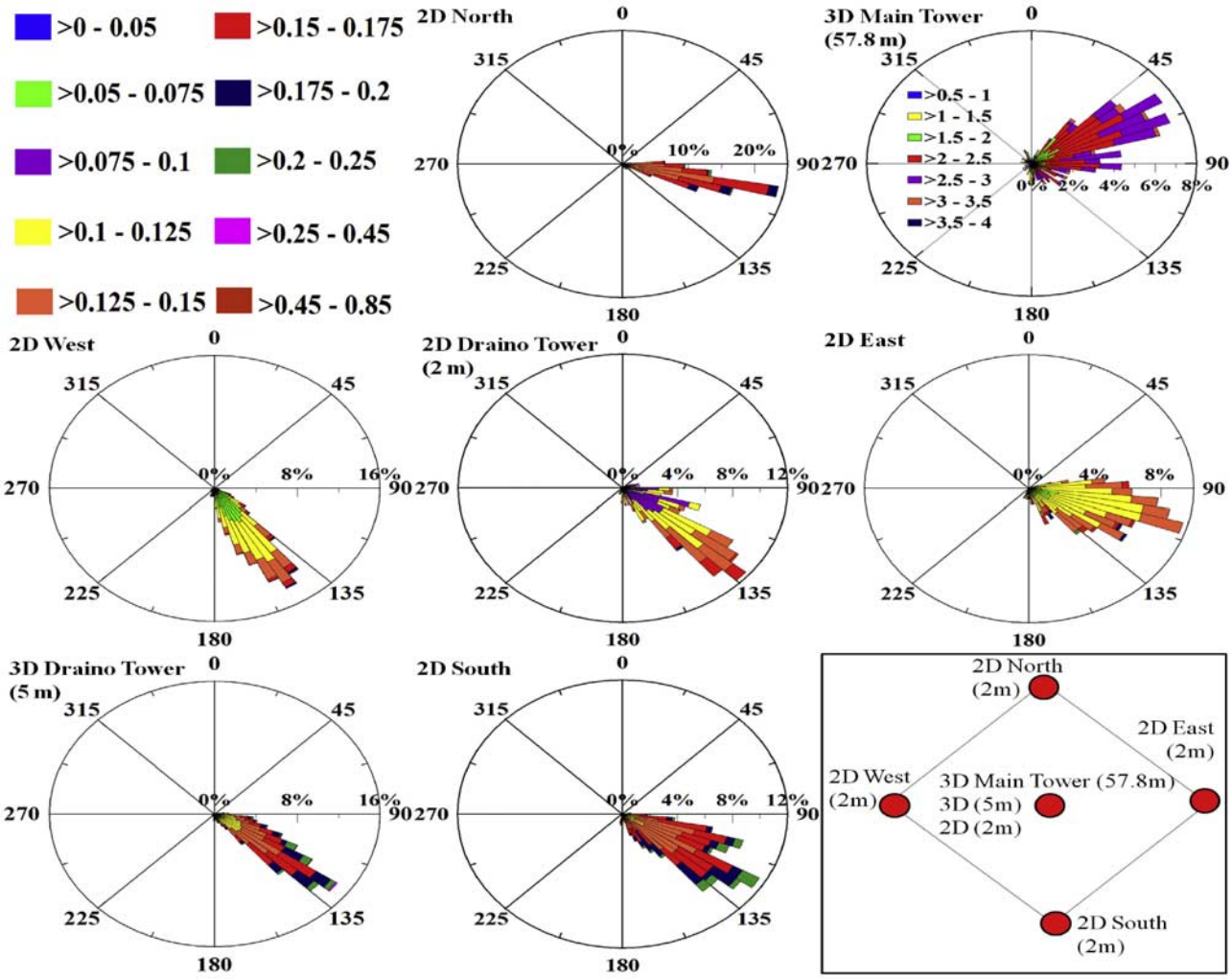

Figure 8. Nighttime distribution of the wind rose and its magnitude (m s^{-1}) for the Draino sonic anemometer network and at top of main tower (57.8 m), including its localization (see Figure 2).

night. There is a persistent wind direction that follows the local topographic gradient (see also Figure 1). These nocturnal horizontal wind directions are in accord with nocturnal wind directions observed at the Jamaraquá station (Figure 1) close to the river Tapajós [*Fitzjarrald et al.*, 2004]. The statistics indicate that the nocturnal horizontal wind magnitude, varies among the subcanopy measurement points, probably due to the large heterogeneity of vegetation structure obstructions [see also *Staebler and Fitzjarrald*, 2004]. The average magnitude of the horizontal wind field in the subcanopy varied from 0.1 to 0.45 m s^{-1}. The observed subcanopy wind direction was prevailing from the southeast, with an interesting shift compared to the top of the main tower (57.8 m) wind direction, indicating a clearly uncoupled situation. Apparently, it seems that the subcanopy flow responds primarily to the local terrain gradients. *Goulden et al.* [2006] have reported a similar shift of the wind direction following the terrain gradient, even at 20 m when compared against the 64 m wind direction (see Figure 6, p. Eight therein). *Sun et al.* [2007] have also indicated that this shift happens at large spatial scales using short-term data sets.

3.3. Subcanopy Flow Forcing Terms

[23] We follow the analysis presented by *Staebler and Fitzjarrald* [2004]. Subcanopy flows are generated by the balance of three driving forces; the pressure gradient perturbations, the buoyancy and the stress divergence, according to the momentum equation. The momentum equation is given by,

$$\frac{\partial u}{\partial t} + u\frac{\partial u}{\partial x} + w\frac{\partial u}{\partial z} = -\frac{1}{\rho}\frac{\partial p'}{\partial x} - g\frac{\theta_v'}{\theta_v}\frac{\partial h}{\partial x} - \frac{\partial \tau}{\partial z},$$

where ρ is the density, p′ the pressure perturbation, θ_v the virtual temperature, θ_v' the local departure of θ_v from the mean, $\frac{\partial h}{\partial x}$ the topographic slope, and τ is the vertical stress, and drag effects are ignored We do not believe that the terrain at the site studied is not so steep as to produce pressure perturbations strong enough to affect subcanopy flow locally, and it is ignored in the subsequent analysis. Thereby, the relative importance of buoyancy ($b_{term} = \left|g\frac{\theta_v'}{\theta_v}\frac{\partial h}{\partial x}\right|$) and stress divergence ($t_{term} = \left|\frac{\partial \tau}{\partial z}\right|$) terms will be considered. Observed

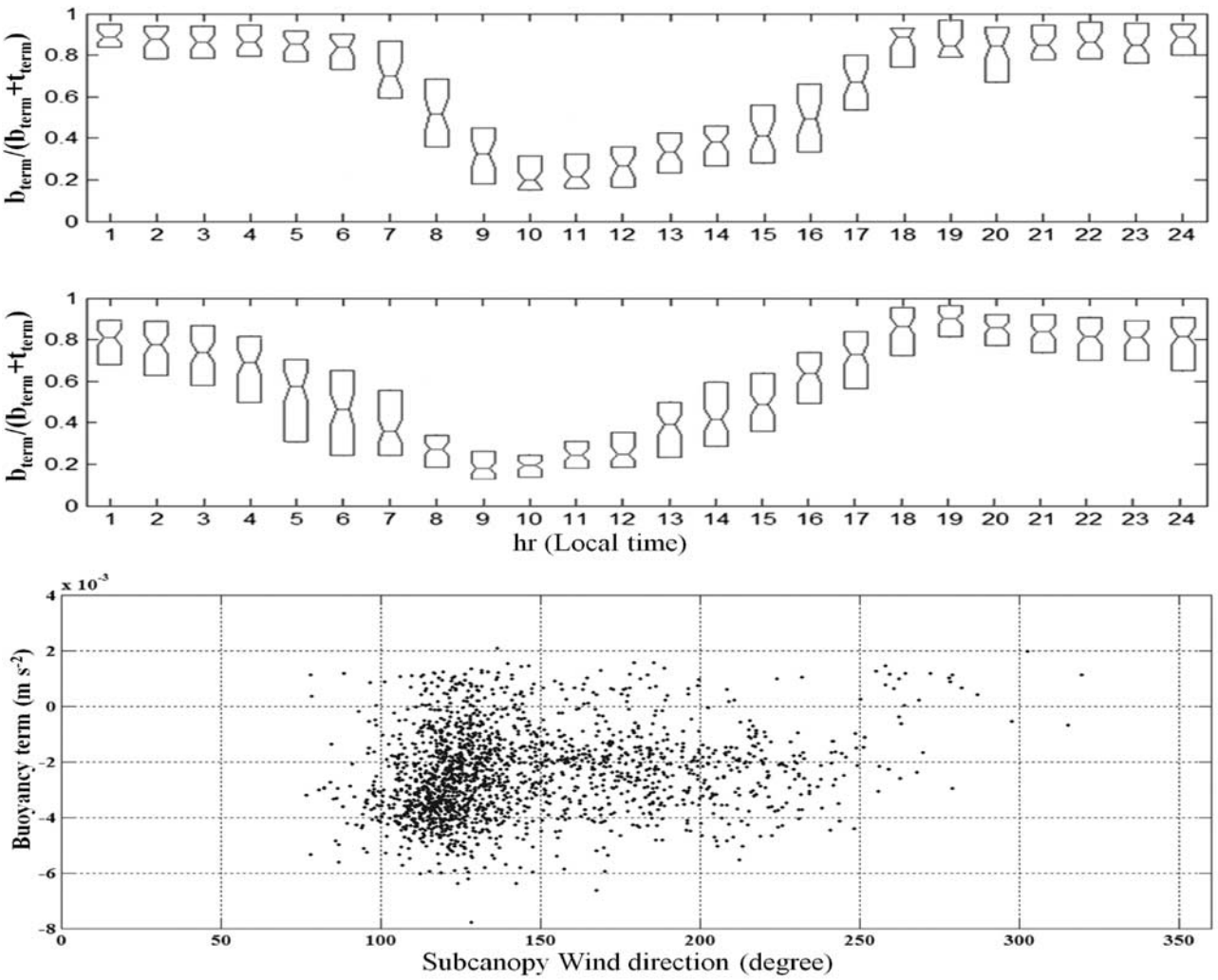

Figure 9. Diurnal cycle of buoyancy term forcing fractions relative to stress divergence term for Phase 1 (top) and Phase 2 (middle) observations, and (bottom) the buoyancy forcing term versus subcanopy wind direction.

fractions of the buoyancy term ($b_{term}/(b_{term} + t_{term})$ and stress divergence term ($t_{term}/(t_{term} + b_{term})$ (Figure 9) indicate that the buoyancy term was more important during the nighttime than was the stress divergence term. The stress divergence term was more significant during the daytime associated with a higher degree of turbulent mixing as expected.

[24] Flows generated by the buoyancy term force the flow down the dominant terrain slope. Nocturnal wind directions were predominantly from the southeast toward northwest, as would be expected given the local topographic gradient (Figure 1). Our observations strongly indicate that the negative buoyancy term is the physical mechanism that explains the nocturnal drainage flow at this relatively flat study site.

3.4. Estimates of Advection Terms

[25] The horizontal advection terms ([2] and [3] in equation (3)) were estimated using subcanopy wind speed components and CO_2 observation data sets from Phase 1 and Phase 2 (14350 and 36459 3-min valid observations, respectively). The horizontal CO_2 gradients were calculated using a linear least squares planar fit (Figure 5). (Note that the interpolated fields shown in Figure 5 were not used in the calculation.)

[26] The hourly time series of average measurement flux terms for the CO_2 budget (Figures 10a and 10b) illustrate that the advective terms and eddy flux are of comparable magnitude, in accordance with recent published results at other sites [*Staebler and Fitzjarrald*, 2004; *Aubinet et al.*, 2005; *Marcolla et al.*, 2005; *Sun et al.*, 2007; *Feigenwinter et al.*, 2008]. Although the advective terms exhibit large scatter, their magnitude is comparable to the other flux terms. When averaged over all periods (for wet and dry phases) we obtained values significantly different from zero. For both phases (dry and wet) at the site studied, indicate a positive contribution to the total flux (i.e., transporting CO_2 out of the control volume around the tower).

[27] The average diurnal cycle of the flux terms for both dry (Phase 1) and wet (Phase 2) periods (Figures 11a and 11b show the expected diurnal eddy flux pattern, negative during the day and positive at night. The vertical advection term plays no important contribution on average, but has a

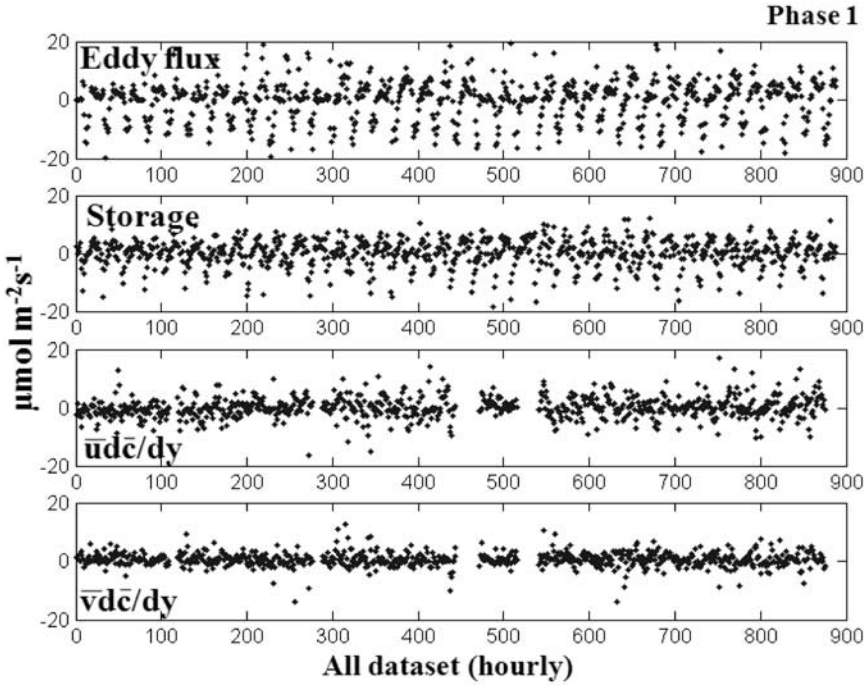

Figure 10a. Hourly averaged summary of results for the Phase 1 and all the terms except eddy flux are average values for 0 to 57.8 m control volume. (top) Vertical eddy flux at 57.8 m; (second panel) storage; (third panel) east-west advection; and (bottom) south-north advection, terms.

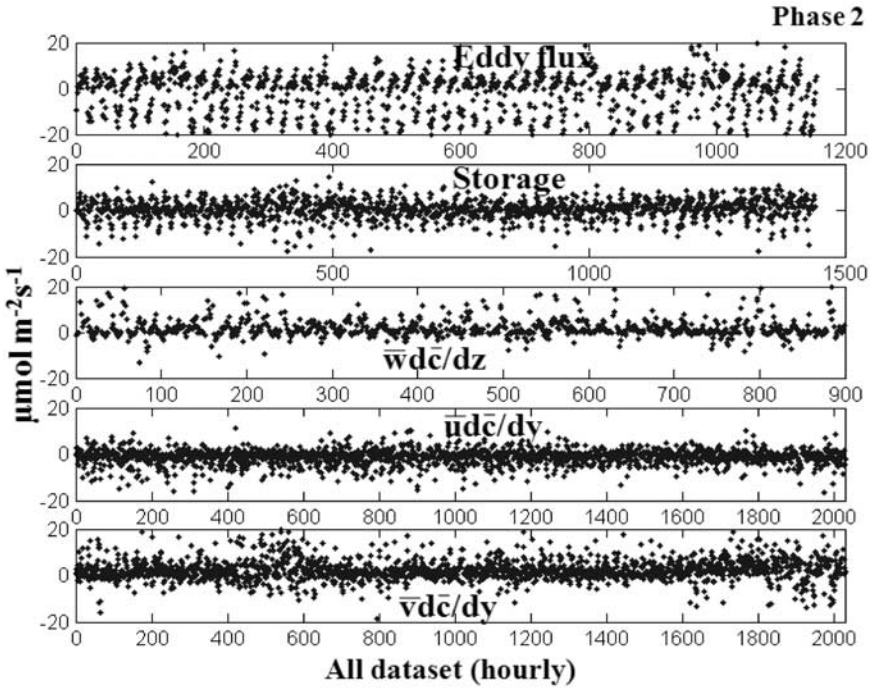

Figure 10b. Hourly averaged summary of results for the Phase 2 and all the terms except eddy flux are average values for 0 to 57.8 m control volume. (top) Vertical eddy flux at 57.8 m; (second panel) storage; (third panel) vertical advection; (fourth panel) east-west advection; and (bottom) south-north advection, terms.

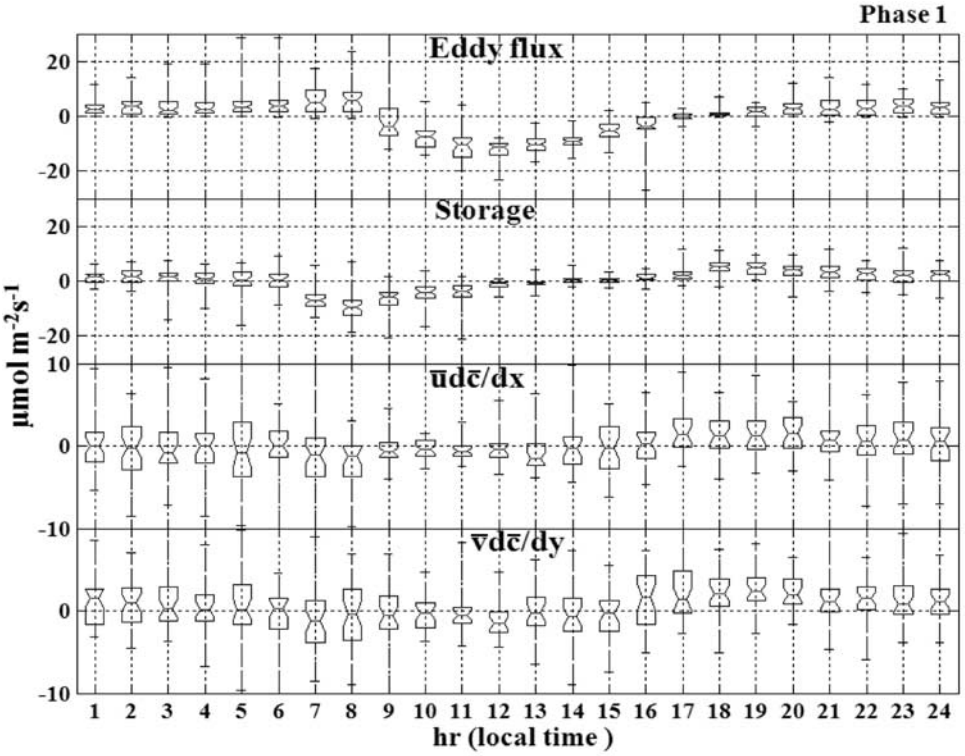

Figure 11a. (top) Hourly averaged vertical eddy flux at 57.8 m; (second panel) storage term; (third panel) east-west advection term; and (bottom) south-north advection, terms. Note the change in vertical scale between the phases.

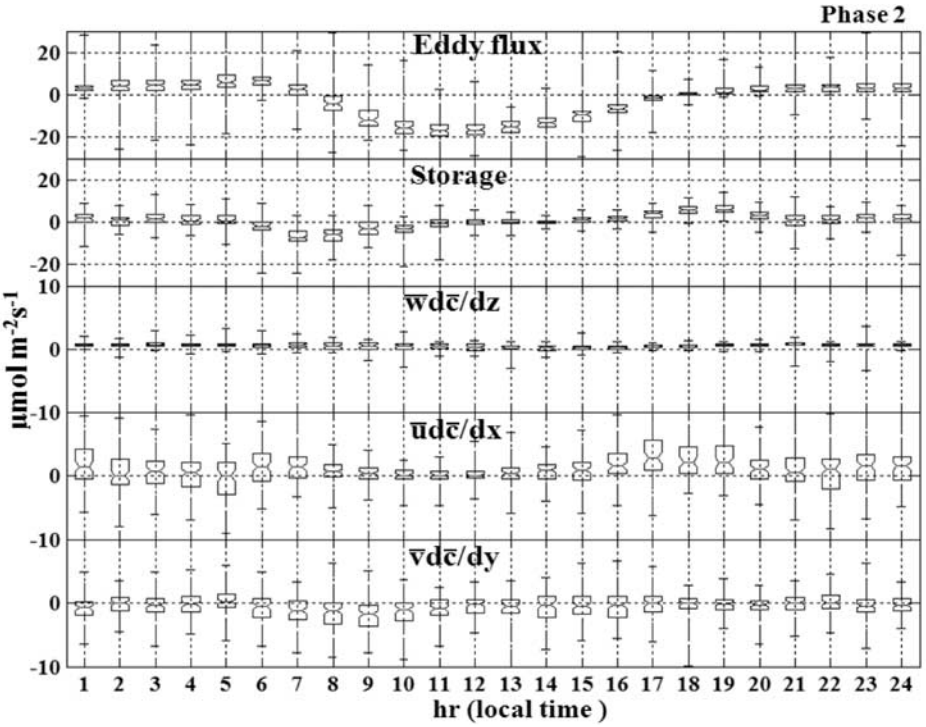

Figure 11b. (top) Hourly averaged vertical eddy flux at 57.8 m; (second panel) storage term; (third panel) vertical advection term; (fourth panel) east-west advection term; and (bottom) south-north advection terms. Note the change in vertical scale between the phases.

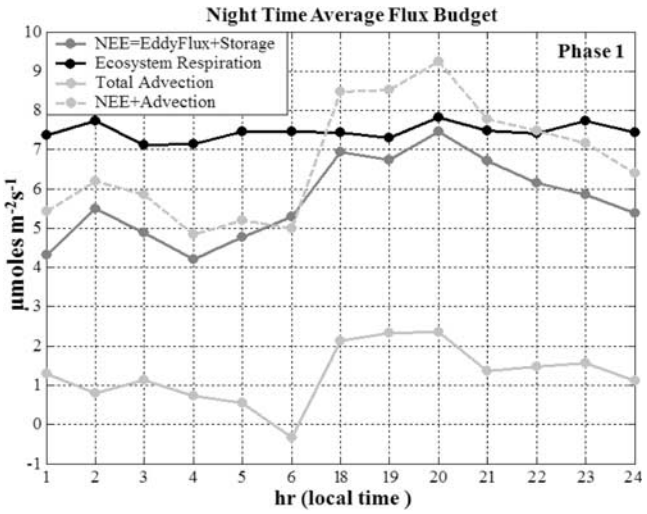

Figure 12a. Mean nocturnal variation of the NEE (eddy covariance flux plus storage), ecosystem respiration, horizontal advection and NEE plus advection, for Phase 1 (dry period).

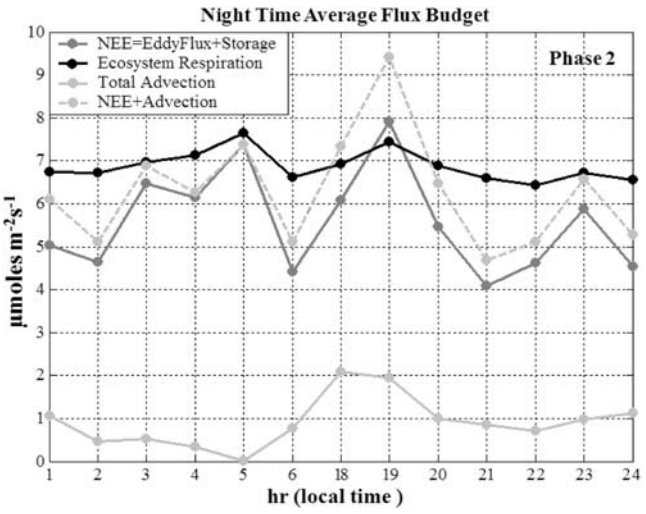

Figure 12b. Same Figure 12a, for Phase 2 (wet period).

positive sign, since the mean vertical velocity and vertical CO_2 gradients were negative. The observed storage term is positive during the night, corresponding to CO_2 buildup in the canopy during stable conditions, and negative in the morning, owing to the release of the accumulated CO_2 due to mixing and onset of photosynthesis.

[28] A notable feature in Figures 11a and 11b is that CO_2 storage during the second part of the night (between 01–06 LT) was 2 to 3 times smaller than the CO_2 storage in first part (between 17–22 LT). This variability might be explained partially by differing CO_2 respiration source intensity from soil, canopy air space stability and canopy structure, but also could have resulted from the drainage flows. Similar patterns were observed by *Yang et al.* [1999] in a Boreal Aspen Forest (USA), see Figure 3 therein. *Aubinet et al.* [2005] made this hypothesis, but did not demonstrate it observationally. It appears that between 1 and 6 LT our observations are consistent with significant positive horizontal advection, transport out of the control volume. The 17–22 LT observations also show positive horizontal advection. However, the high ecosystem respiration rate maintains a large storage term, and this partially offsets this horizontal advection in the CO_2 budget.

3.5. CO_2 Budget

[29] To determine the relative contribution of the nocturnal advection terms to the CO_2 budget, we compare the mean nocturnal variation of NEE (eddy flux + storage) with and without considering the observed advection terms and ecosystem respiration during dry (Phase 1) and wet (Phase 2) periods of observation (Figures 12a and 12b). The ecosystem respiration, EC flux, and storage were measured by the CD-10 group [*Saleska et al.*, 2003; *Hutyra et al.*, 2007]. Results show that the differences between NEE and ecosystem respiration are improved when the advection term is accounted for (Table 2 and Figures 12a and 12b). The advection term accounts for 1.27 μmol m^{-2} s^{-1} and 0.91 μmol m^{-2} s^{-1}, for Phase 1 and Phase 2 respectively, representing 71% and 73% of the observational 'deficit' between ecosystem respiration and NEE.

3.6. Correlation Between Advection Components and Friction Velocity

[30] For the site studied here, the threshold value for friction velocity [e.g., *Falge et al.*, 2001; *Gu et al.*, 2005] was reported by *Saleska et al.* [2003] and *Miller et al.* [2004] to be between 0.2 and 0.3 m s^{-1}. Is the assumption that advection is only significant below this threshold valid? Our results show a clear dependence of the advection term on friction velocity for both observation periods (Figure 13). There is a significant positive advection contribution to the CO_2 budget that should be included in the NEE calculation, even when the friction velocity is higher than the threshold values commonly used. Our results in the Tapajós forest indicate that this interval lies between 0.3 and 0.6 m s^{-1}.

4. Summary and Conclusions

[31] We present results of the first effort to determine observationally the importance of the nocturnal advection processes on the CO_2 budget in the Amazon tropical rain forest. We tested the hypothesis that persistent nocturnal subcanopy horizontal advection exists and transports an important amount of CO_2 out of the control volume at one old-growth tropical rain forest site. We determined the magnitude of the horizontal subcanopy gradients of CO_2 and of the wind field and found sufficient net horizontal advection to affect the CO_2 budget.

Table 2. Summary of Mean Nocturnal CO_2 Budget for Phase 1 and Phase 2

Flux Components (μmol m^{-2} s^{-1})	Phase 1	Phase 2
NEE	5.71	5.58
Respiration	7.45	6.87
Deficit	1.74	1.29
Advection	1.27	0.91
NEE + Advection	6.98	6.49

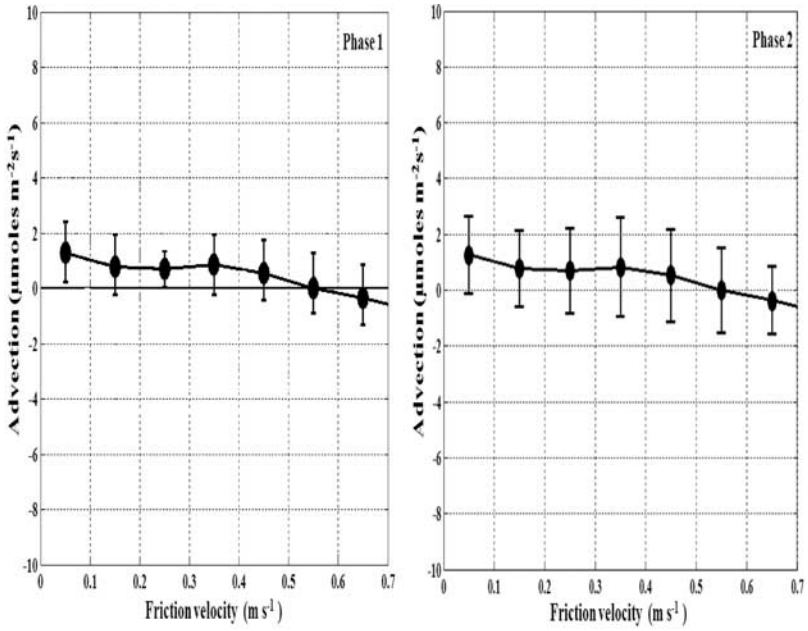

Figure 13. Mean nocturnal variation of the advection term as a function of the friction velocity rank, for Phase 1 (left) and Phase 2 (right) data sets. Solid line with dots indicates binned average values (0.1 intervals)). Error bar also is plot with standard deviation, respectively.

[32] The methodology established by *Staebler and Fitzjarrald*, 2004, 2005] was applied and tested to measure the subcanopy scalar gradients and wind field. These data were complemented by eddy flux and mean profile observations made at the same site on a 65-m tower (section 2). The measurements were performed in the dry season (DOY 198–238 2003 - Phase 1) and in the wet season (DOY 278–366 2004 and 1–32 2005 - Phase 2). The horizontal gradient of the CO_2 concentration and average wind speed, were on the order of 0.02 ppm m^{-1} and 0.12 m s^{-1}, respectively (section 3.1).

[33] Prevailing subcanopy wind directions were from the southeast and were well correlated with gentle undulations of the landscape near the tower. The tropical forest subcanopy near the forest floor was stable at all times of day, but it was more pronounced during all 130 selected nights analyzed (section 3.2). That there was little coupling with the flow aloft indicates that there is potential for lateral export of subcanopy CO_2 even during the daytime, when this effect is often ignored. The negative buoyancy term was the principal physical mechanism responsible for generating the nocturnal subcanopy flow. During the daytime the stress divergence term was dominant, suppressing the dominance of the buoyancy effect (section 3.3).

[34] The results from direct measurements of the horizontal gradients of CO_2 and wind speed components measured in the subcanopy indicated that its magnitudes were sufficiently significant to produce a net nocturnal horizontal advection average between 0.91 and 1.27 μmol m^{-2} s^{-1} for dry and wet observation periods, respectively. Nocturnal horizontal advection was of the same order as the vertical EC and storage flux components. Depletion of the storage component was due in large part to net positive horizontal advection, primarily during the second part of the night (01–06 LT; section 3.4).

[35] Comparison of the nocturnal deficit from ecosystem respiration and NEE measured on the eddy flux tower demonstrated the important contribution of the mean nocturnal horizontal advection on the atmospheric CO_2 budget. The mean nocturnal advection component represented 73% and 71% of this deficit for dry and wet periods analyzed (130 nights), respectively.

[36] This suggests an important role of the nocturnal advection for the total CO_2 budget at this site. It was also verified that for nighttime intervals, with friction velocity between 0.3 and 0.6 m s^{-1} (commonly accepted as sufficient to provide correct nighttime eddy fluxes), there was a positive net horizontal transport of CO_2 by the advection component. Therefore, even under considerable high turbulence levels at night, horizontal advection transport in the total CO_2 budget is significant.

[37] These results confirm that few sites are flat enough that horizontal advective effects can be ignored a priori. In future work the validity of the CO_2 profile similarity hypothesis we invoked to introduce shape factors in (4) should be linked explicitly to the observed mean vegetation profile. Observational estimates of the effect of mean vertical velocity on scalar budgets may be the major source of uncertainty in the budget. Continuous, long-term observations with redundant instrumentation are needed to clarify this issue.

[38] **Acknowledgments.** This work is part of the LBA-ECO project, supported by the NASA Terrestrial Ecology Branch under grants NCC5-283 and NNG-06GE09A to the Atmospheric Sciences Research Center, University at Albany, SUNY, LBA-ECO team CD-03. The latter grant included a subcontract to the Fundação Djalma Batista, Manaus. Julio Tóta was also supported by FAPEAM RH-POSGRAD during 2007 and by MCT-INPA-Fundação Djalma Batista during 2006–2007, with a fellowship. Thanks to V. Miranda and E. Brait for help during the field work. Thanks to Scott Saleska and CD-10 LBA-ECO group for flux-tower data and to Edwin

Keizer for SRTM data and plots. Detailed comments and suggestions from anonymous reviewers and the editors greatly improved the manuscript.

References

Araújo, A. C., et al. (2002), Comparative measurements of carbon dioxide fluxes from two nearby towers in a central Amazonian rainforest: The Manaus LBA site, *J. Geophys. Res.*, *107*(D20), 8090, doi:10.1029/2001JD000676.

Aubinet, M., et al. (2000), Estimates of the annual net carbon and water exchange of forests: The EUROFLUX methodology, *Adv. Ecol. Res.*, *30*, 113–175.

Aubinet, M., B. Heinesch, and M. Yernaux (2003), Horizontal and vertical CO_2 advection in a sloping forest, *Boundary Layer Meteorol.*, *108*(3), 397–417.

Aubinet, M., et al. (2005), Comparing CO_2 storage and advection conditions at night at different Carboeuroflux sites, *Boundary Layer Meteorol.*, *116*, 63–94.

Baldocchi, D. D., B. B. Hicks, and T. P. Meyers (1988), Measuring biosphere-atmosphere exchanges of biologically related gases with micrometeorological methods, *Ecology*, *69*(5), 1331–1340.

Baldocchi, D., J. Finnigan, K. Wilson, and E. Falge (2000), On measuring net ecosystem carbon exchange over tall vegetation on complex terrain, *Boundary Layer Meteorol.*, *96*(1–2), 257–291.

Baldocchi, D., et al. (2001), FLUXNET: A new tool to study the temporal and spatial variability of ecosystem-scale carbon dioxide, water vapor, and energy flux densities, *Bull. Am. Meteorol. Soc.*, *82*(11), 2415–2434.

Black, T. A., et al. (1996), Annual cycles of water vapour and carbon dioxide fluxes in and above a boreal aspen forest, *Global Change Biol.*, *2*(3), 219–229.

Clark, D. B. (1996), Abolishing virginity, *J. Trop. Ecol.*, *12*, 735–739.

da Rocha, H. R., M. L. Goulden, S. D. Miller, M. C. Menton, L. D. V. O. Pinto, H. C. de Freitas, and A. M. E. S. Figueira (2004), Seasonality of water and heat fluxes over a tropical forest in eastern Amazonia, Ecol, *Appl.*, *14*(4, suppl. S), S22–S32.

Falge, E., et al. (2001), Gap filling strategies for defensible annual sums of net ecosystem exchange, *Agric. For. Meteorol.*, *107*, 43–69.

Feigenwinter, C., C. Bernhofer, and R. Vogt (2004), The influence of advection on the short term CO_2-budget in and above a forest canopy, *Boundary Layer Meteorol.*, *113*(2), 201–224.

Feigenwinter, C. C., et al. (2008), Comparison of horizontal and vertical advective CO_2 fluxes at three forest sites, *Agric. For. Meteorol.*, *145*, 1–21.

Fitzjarrald, D. R., and K. E. Moore (1990), Mechanisms of nocturnal exchange between the rain-forest and the atmosphere, *J. Geophys. Res.*, *95*(D10), 16,839–16,850.

Fitzjarrald, D. R., K. E. Moore, O. M. R. Cabral, J. Scolar, A. O. Manzi, and L. D. D. Sa (1990), Daytime turbulent exchange between the Amazon Forest and the atmosphere, *J. Geophys. Res.*, *95*(D10), 16,825–16,838.

Fitzjarrald, D. R., R. K. Sakai, O. L. L. Moraes, M. J. Czikowsky, O. C. Acevedo, and R. C. Oliveira (2004), Mesoclimate of the LBA-ECO Santarém study area, paper presented at III LBA Scientific Conference, Braz. Minist. of Sci. and Technol., Brasilia, Brazil, July.

Goulden, M. L., J. W. Munger, S. M. Fan, B. C. Daube, and S. C. Wofsy (1996), Measurements of carbon sequestration by long-term eddy covariance: Methods and a critical evaluation of accuracy, *Global Change Biol.*, *2*(3), 169–182.

Goulden, M. L., S. D. Miller, H. R. da Rocha, M. C. Menton, H. C. de Freitas, A. M. E. S. Figueira, and C. A. D. de Sousa (2004), Diel and seasonal patterns of tropical forest CO_2 exchange, *Ecol. Appl.*, *14*(4, suppl. S), S42–S54.

Goulden, M. L., S. D. Miller, and H. R. da Rocha (2006), Nocturnal cold air drainage and pooling in a tropical forest, *J. Geophys. Res.*, *111*, D08S04, doi:10.1029/2005JD006037.

Gu, L., E. Falge, T. Boden, D. D. Baldocchi, T. A. Black, S. R. Saleska, T. Suni, T. Vesala, S. Wofsy, and L. Xu (2005), Observing threshold determination for nighttime eddy flux filtering, *Agric. For. Meteorol.*, *128*, 179–197.

Hutyra, L. R., J. W. Munger, S. R. Saleska, E. Gottlieb, B. C. Daube, A. L. Dunn, D. F. Amaral, P. B. de Camargo, and S. C. Wofsy (2007), Seasonal controls on the exchange of carbon and water in an Amazonian rain forest, *J. Geophys. Res.*, *112*, G03008, doi:10.1029/2006JG000365.

Keller, M., et al. (2004), Ecological research in the large-scale biosphere atmosphere experiment in Amazonia: Early results, *Ecol. Appl.*, *14*(4, suppl. S), S3–S16.

Kruijt, B. J., A. Elbers, C. von Randow, A. C. Arau'jo, P. J. Oliveira, A. Culf, A. O. Manzi, A. D. Nobre, P. Kabat, and E. J. Moors (2004), The robustness of eddy correlation fluxes for Amazon rain forest conditions, *Ecol. Appl.*, *14*(suppl. S), S101–S113.

Lee, X. H. (1998), On micrometeorological observations of surface-air exchange over tall vegetation, *Agric. For. Meteorol.*, *91*(1–2), 39–49.

Malhi, Y., A. D. Nobre, J. Grace, B. Kruijt, M. G. P. Pereira, A. Culf, and S. Scott (1998), Carbon dioxide transfer over a central Amazonian rain forest, *J. Geophys. Res.*, *103*, 31,593–31,612.

Marcolla, B., A. Cescatti, L. Montagnani, G. Manca, G. Kerschbaumer, and S. Minerbi (2005), Importance of advection in the atmospheric CO_2 exchanges of an alpine forest, *Agric. For. Meteorol.*, *130*, 193–206.

Miller, S. D., M. L. Goulden, M. C. Menton, H. R. da Rocha, H. C. de Freitas, A. M. E. S. Figueira, and C. A. D. de Sousa (2004), Biometric and micrometeorological measurements of tropical forest carbon balance, *Ecol. Appl.*, *14*(4, suppl. S), S114–S126.

Parker, G., and D. R. Fitzjarrald (2004), Canopy structure and radiation environment metrics indicate forest developmental stage, disturbance, and certain ecosystem functions, paper presented at III LBA Scientific Conference, Braz. Minist. of Sci. and Technol., Brasilia, Brazil, July.

Parotta, J. A., J. K. Franci, and R. R. de Almeida (1995), Trees of the Tapajos: A photographic field guide, *Gen. Tech. Rep. IITF-1*, 371 pp., U.S. Dep. of Agric., Rio Piedras, Puerto Rico.

Paw U, K. T., D. D. Baldocchi, T. P. Meyers, and K. B. Wilson (2000), Correction of eddy covariance measurements incorporating both advective effects and density fluxes, *Boundary Layer Meteorol.*, *97*, 487–511.

Saleska, S. R., et al. (2003), Carbon in Amazon forests: Unexpected seasonal fluxes and disturbance-induced losses, *Science*, *302*(5650), 1554–1557.

Silver, W. L., et al. (2000), Effects of soil texture on belowground carbon and nutrient storage in a lowland Amazonian forest ecosystem, *Ecosystems (N.Y., Print)*, *3*, 193–209.

Staebler, R. M. (2003), Forest subcanopy flows and micro-scale advection of carbon dioxide, Ph.D. dissertation, State Univ. of N. Y., Albany.

Staebler, R. M., and D. R. Fitzjarrald (2004), Observing subcanopy CO_2 advection, *Agric. For. Meteorol.*, *122*(3–4), 139–156.

Staebler, R. M., and D. R. Fitzjarrald (2005), Measuring canopy structure and kinematics of subcanopy flows in two forests, *J. Appl. Meteorol.*, *44*, 1161–1179.

Sun, J., S. P. Burns, A. C. Delany, S. P. Oncley, A. A. Turnipseed, B. B. Stephens, D. H. Lenschow, M. A. LeMone, R. K. Monson, and D. E. Anderson (2007), CO_2 transport over complex terrain, *Agric. For. Meteorol.*, *145*, 1–21.

Turnipseed, A. A., D. E. Anderson, P. Blanken, W. M. Baugh, and R. K. Monson (2003), Airflows and turbulent flux measurements in mountainous terrain. Part 1. Canopy and local effects, *Agric. For. Meteorol.*, *119*, 1–21.

Vickers, D., and L. Mahrt (2006), Contrasting mean vertical motion from tilt correction methods and mass continuity, *Agric. For. Meteorol.*, *138*, 93–103.

Yang, P. C., T. A. Black, H. H. Neumann, M. D. Novak, and P. D. Blanken (1999), Spatial and temporal variability of CO_2 concentration and flux in a boreal aspen forest, *J. Geophys. Res.*, *104*(D22), 27,653–27,661.

Yi, C., K. J. Davis, P. S. Bakwin, B. W. Berger, and L. Marr (2000), The influence of advection on measurements of the net ecosystem-atmosphere exchange of CO_2 from a very tall tower, *J. Geophys. Res.*, *105*, 9991–9999.

Yoshino, M. M. (1984), Thermal belt and cold air drainage on the mountain slope and cold air lake in the basin at quiet, clear night, *GeoJournal*, *8*(3), 235–250.

O. C. Acevedo and O. M. M. Moraes, Departamento de Física, Universidade Federal de Santa Maria, Santa Maria, Rio Grande do Sul 97105-900, Brazil.

D. R. Fitzjarrald and R. K. Sakai, Atmospheric Sciences Research Center, University at Albany, State University of New York, Albany, NY 12203, USA.

A. O. Manzi and J. Tóta, Instituto Nacional de Pesquisas da Amazônia, Manaus, Amazonas 69060-001, Brazil. (tota@inpa.gov.br)

R. M. Staebler, Air Quality Research Branch, Environment Canada, Toronto, ON M3H 5T4, Canada.

S. C. Wofsy, Department of Earth and Planetary Sciences, Harvard University, Cambridge, MA 02138, USA.